NEOPLASIA
www.neoplasia.com
Volume 14 Number 4 April 2012 pp. 271–282 271

Transgenic Overexpression of the Proprotein Convertase Furin Enhances Skin Tumor Growth[1]

Jian Fu*,†, Daniel E. Bassi*,†, Jirong Zhang*,†, Tianyu Li‡, Emmanuelle Nicolas§ and Andres J.P. Klein-Szanto*,†

*Department of Pathology, Fox Chase Cancer Center, Philadelphia, PA, USA; †Cancer Biology Program, Fox Chase Cancer Center, Philadelphia, PA, USA; ‡Bioinformatics and Biostatistics Facility, Fox Chase Cancer Center, Philadelphia, PA, USA; §Genomics Facility, Fox Chase Cancer Center, Philadelphia, PA, USA

Abstract

Furin, one of the members of the family of proprotein convertases (PCs), ubiquitously expressed as a type I membrane-bound proteinase, activates several proteins that contribute to tumor progression. *In vitro* studies using cancer cell lines and clinical specimens demonstrated that furin processes important substrates such as insulin-like growth factor 1 receptor (IGF-1R) and transforming growth factor β, leading to increased tumor growth and progression. Despite the numerous studies associating furin with tumor development, its effects in preclinical models has not been comprehensively studied. In this study, we sought to determine the protumorigenic role of furin *in vivo* after a two-stage chemical carcinogenesis protocol in transgenic mice in which furin expression was targeted to the epidermal basal layer. We found that processing of the PC substrate IGF-1R and the proliferation rate of mouse epidermis was enhanced in transgenic mice when compared with their WT counterparts. Histopathologic diagnoses of the tumors demonstrated that furin transgenic mice (line F47) developed twice as many squamous carcinomas as the control, WT mice ($P < .002$). Similarly, tumors cells from transgenic mice were able to process PC substrates more efficiently than tumor cells from WT mice. Furthermore, furin expression resulted in a higher SCC volume in transgenic mice as well as an increase in the percentage of high-grade SCC, including poorly differentiated and spindle cell carcinomas. In conclusion, expression of furin in the basal layer of the epidermis increased tumor development and enhanced tumor growth, supporting the consideration of furin as a potential target for cancer treatment.

Neoplasia (2012) 14, 271–282

Introduction

The family of proprotein convertase (PC) is composed of a group of serine proteinases implicated in regulating a broad range of complex physiological and pathologic processes [1,2] by proteolytic activation of precursor proteins. Nine members have already been identified, including PC1/3, PC2, furin, PC4, PC5/6, PACE4, PC7, SKI-1/S1P, and PCSK9 [3–5]. Most of these enzymes exert their functions by processing numerous precursor protein substrates cleaving them at basic residues within the motif (K/R)-$(X)_n$-(K/R), where n = 0, 2, 4, or 6 and where K is lysine, R is arginine, and X is any amino acid except cysteine. Some of the PC protein substrates such as growth factors and their cognate receptors, metalloproteinases, and adhesion molecules are highly relevant to the neoplastic cell behavior [6–18]; therefore, many attempts were made to explore the involvement of PCs in tumor growth and development. Several studies demonstrated that PC1, PC2, furin, PC5, PACE4, and PC7 are involved in regulating the biologic behavior of various types of tumors [19–22]. Specifically, furin, a ubiquitously expressed type I membrane-bound proteinase, has been reported to be implicated in tumors of different origins. Furin messenger RNA was elevated in lung non–small cell carcinoma but not in small cell

Abbreviations: DMBA, 7, 12-dimethylbenz[*a*]anthracene; F47, furin transgenic mouse line number 47; F49, furin transgenic mouse line number 49; PC, proprotein convertase; SCC, squamous cell carcinoma; TPA, 12-*O*-tetradecanoylphorbol-13-acetate; WT, wild-type

Address all correspondence to: Andres J.P. Klein-Szanto, MD, PhD, Department of Pathology, Fox Chase Cancer Center, 333 Cottman Ave, Philadelphia, PA 19111.
E-mail: aj_klein-szanto@fccc.edu

[1]This work was supported by grants from the National Institutes of Health CA133001, CA06927 and by an appropriation from the Commonwealth of Pennsylvania.
Received 12 January 2012; Revised 2 April 2012; Accepted 2 April 2012

DOI 10.1593/neo.12166

carcinoma [23,24]. In human head and neck squamous cell carcinomas (HNSCCs), furin expression and activity correlated with tumor progression based on the facts that furin messenger RNA and protein were detected only in aggressive and metastasizing tumors [25,26].

Coexpression of insulin-like growth factor 1 receptor (IGF-1R) with different PCs in furin-defective LoVo-C5 cells demonstrated that furin is one of the major PCs responsible for pro–IGF-1R activation [8]. Stable expression of α_1-antitrypsin Portland (PDX), a potent competitive inhibitor of furin, resulted in the reduction of DNA synthesis, anchorage-independent growth, and enhanced apoptotic phenotype [27] and decreased tumorigenesis of xenotransplanted human tumor cells [28]. Moreover, furin processed platelet-derived growth factor A and vascular endothelial growth factor C. This regulatory ability was tightly associated with tumorigenesis and metastasis in tumor cell models [29–31]. Furthermore, expression of its naturally occurring prosegment inhibitor, ppFurin in cancer cell lines, contributed to decreased matrix metalloproteinase MMP-9 activity, cell motility, migration, and invasion of collagen [32] as well as activation of platelet-derived growth factor A [33].

Our group found significant decrease or absence of tumorigenicity after subcutaneous inoculation of tumor cells into severe combined immunodeficient mice by transfecting PDX into HNSCC or astrocytoma cells [25,34]. The furin substrates IGF-1R, transforming growth factor β (TGF-β), and membrane type 1–matrix metalloprotease were not activated in PDX-expressing cells. This PDX-mediated tumor suppression is mostly attributed to furin inhibition because tumor cells expressing ppFur showed a similar loss or decrease in their tumorigenic ability [28]. Furthermore, overexpression of furin caused a significant increase in the invasive potential of HNSCC cells of low and moderate aggressive potential *in vitro* and *in vivo* [27]. A synthetic furin inhibitor, decanoyl-Arg-Val-Lys-Arg-chloromethyl-ketone (CMK) eliminated the inhibitory effect of furin in the same tumor cells [27].

These successful *in vitro* and xenotransplantation experiments stimulated the development of a mouse model to evaluate the effects of PCs activity *in vivo*. Using a transgenic mouse model, we investigated the function of another tumor-associated PC, PACE4 targeted to the epidermis, in the processes of mouse skin squamous cell carcinoma (SCC) growth and progression [35]. PACE4 transgenic mice developed twice as many tumors as the wild-type (WT) counterpart and showed significant disruptions of the basement membrane (BM), increasing the invasive and metastatic behavior of the chemically induced SCCs. However, PACE4's role in tumor proliferation was less impressive. Furin, on the other hand, has a prominent role in the processing of IGF-1R, an antiapoptotic and proproliferative substrate. In this context, its effects on tumor cell proliferation may be more pronounced than PACE4's. To study the role of furin in skin proliferation and carcinogenesis, we developed another transgenic mouse model that expresses furin in the epidermal basal layer and treated the mice with a two-stage carcinogenesis protocol to ascertain the effect of this PC on tumor development and progression.

Materials and Methods

Materials

12-*O*-Tetradecanoylphorbol-13-acetate (TPA) and 7, 12-dimethylbenz (*a*)anthracene (DMBA) were purchased from Sigma-Aldrich (St Louis, MO). FVB/N mice, 6 to 8 weeks of age, were purchased from Taconic (Germantown, NY) and were used as WT controls.

Generation and Identification of K5-Furin Mice

The 3.2-kb full-length WT human furin complementary DNA (cDNA) was excised from its parental pcDNA3.1 vector using *Pme*I and *Eco*RV. The blunt-ended fragment was ligated into the *Sna*BI site between the rabbit β-globin intron and the polyadenylation sequences from a vector described previously [35] and inserted into the K5 expression vector. Orientation and integrity of the insert were confirmed by restriction analysis and sequencing. The K5-furin construct was microinjected into the pronuclei of mouse embryos obtained from FVB female mice mated with FVB male mice. DNA was extracted from clipped tails as described [35]. Mice were genotyped by polymerase chain reaction (PCR) analysis of tail DNA using primers specific for an internal fragment of furin and the junction of furin with SV40 polyadenylation signal. The sequence of sense primer was 5′GTGCTGTCTCATCGATTTGGCAA3′ and that of antisense primer was 5′GCGGGCGGTGAGGCGACA3′ [36].

Tumor Induction Experiments

The two-stage carcinogenesis protocol was as follows: a single 100-nmol initiating dose of DMBA in 0.2 ml of acetone was applied topically to the shaved dorsal skin of 6- to 8-week-old female mice. One week after DMBA treatment, TPA (4 nmol) in 0.2 ml of acetone was applied twice weekly to the skin for the duration of the experiment (30 weeks). Tumor incidence and multiplicity were observed weekly starting at 8 weeks of TPA promotion. The number of mice per group was as follows: 33 WT mice, 28 K5-Furin line 47 (F47) mice, and 30 K5-Furin line 49 (F49) mice. Papillomas and SCCs were recorded by gross observation and confirmed by histologic analysis (see next paragraphs). Autopsies of carcinoma-bearing mice were performed, and metastases in axial lymph nodes, lung, liver, spleen, and other organs were recorded. All tumors were analyzed histologically. SCCs were classified according to histopathologic grade [37]. Most SCCs were endophytic growths that invaded the dermis and subcutaneous tissue. The differentiation patterns defining the histopathologic grade were as follows: 1) grade 1 SCC, very well differentiated with most of the tumor containing keratinizing cells and horny pearls; 2) grade 2 SCC, moderately differentiated tumors in which up to 50% of the tumor mass is formed by keratinizing cells; 3) grade 3 SCC or poorly differentiated tumors, containing less than 25% tumor mass showing evidence of keratinization; and 4) grade 4 SCCs, very poorly differentiated tumors or spindle cell carcinomas containing very little or no histologic evidence of keratinization.

Keratinocyte Cultures and Western Blot Analyses

Primary epidermal keratinocytes from newborn mice were used to determine expression levels of furin because of their suitability for *in vitro* growth and further molecular analyses. Primary epidermal keratinocytes were established *in vitro* as described [38,39]. Briefly, 1- to 3-day-old mice were euthanized, the skin was washed in a 1:10 solution of povidone-iodine (Betadine; Purdue Pharma, Stamford, CT), and rinsed twice in sterile dH_2O and twice in 70% alcohol. The skin was removed and floated overnight on 2 ml of dispase (Dispase II, 25 U/ml; BD Biosciences, Bedford, MA). The epidermis was separated from the dermis, minced and incubated with 2 ml of 0.05% trypsin and 0.01% EDTA for 20 minutes at 37°C. DNase I (100 U) was added, and the cells were mechanically dissociated by vigorous pipetting followed by filtration through a 40-μm cell strainer (BD Biosciences). The cells were washed in Dulbecco modified Eagle medium containing

10% fetal calf serum and plated in low-Ca^{2+} keratinocyte growth medium (Ca^{2+}-free KGM 1:2; Cambrex, Walkersville, MD).

The keratinocytes grown in culture dishes were lysed and subjected to furin Western blot analysis according to our previously reported protocol [40]. The monoclonal antibody against furin (MON-152, ALX-803-017; ALEXIS, Plymouth Meeting, PA) that recognizes human furin was used as the primary antibody.

The processing of IGF-1R in keratinocytes was performed by culturing keratinocytes to 80% to 90% confluence and subsequently treating cells with furin convertase inhibitor, CMK (Val-Lys-Arg-chloromethylketone, ALX-260-022; Enzo Life Sciences, Plymouth Meeting, PA) at different concentrations. Twenty-four hours after CMK treatment, the keratinocytes were lysed and subjected to Western blot analysis with polyclonal antibody against IGF-1Rβ (C-20, sc-713; Santa Cruz Biotechnologies, Santa Cruz, CA). Primary tumors derived from mice were also studied for expression of IGF-1Rβ and TGF-β (no. 555052; BD Pharmingen, San Diego, CA) by Western blot analysis. The quantification of Western blot results was performed by using ImageJ developed by the National Institutes of Health.

Analysis of Epidermal Thickness and Cell Proliferation after Treatment with TPA

To evaluate whether furin expression alters the proliferative ability of the epidermis, we compared the proliferative response to the topically applied phorbol ester TPA on the dorsal skin of WT and transgenic animals. Groups of WT or furin transgenic mice (n = 5) were treated with two applications of TPA (5 nmol) in acetone (acetone alone was applied to a control group) separated by 48 hours and euthanized the mice 48 hours after the last treatment. Paraffin sections were stained with hematoxylin and eosin, and the skin thickness was measured with a morphometry software that permits length measurements using digital imaging (Image Pro-Plus; Media Cybernetics, Silver Spring, MD). For analysis of cell proliferation, paraffin sections were used for detecting the proliferation marker Ki67, using a rat monoclonal antibody (clone TEC-3; Dako, Carpinteria, CA) and a biotinylated goat anti-rat IgG antibody (mouse adsorbed) together with an ABC detection kit (Vector Elite; Vector, Burlingame, CA). Slides were mounted and observed with a Nikon Optiphot (Nikon Instruments, Inc, Melville, NY) with a Plan/Apo objective 20×, NA, 0.75, Nikon eyepiece ×10, final magnification ×200. Epidermal cell proliferation index was determined in the interfollicular and intrafollicular epidermis by scanning the slides using an Aperio CS ScanScope scanner (Aperio, Vista, CA) and counting Ki67-positive and Ki67-negative epidermal basal keratinocytes and determining the percentage of positive cells (three to five mice per group; minimum number of cells counted/mouse was 500 per mouse).

Immunohistochemistry of Furin

Furin immunohistochemistry was performed using paraffin-embedded normal skin, normal internal organs, and cutaneous tumors from WT and transgenic mice. All paraffin sections were subjected to a previously published immunostaining protocol [37,41]. A monoclonal antibody against furin that detects mouse and human furin protein

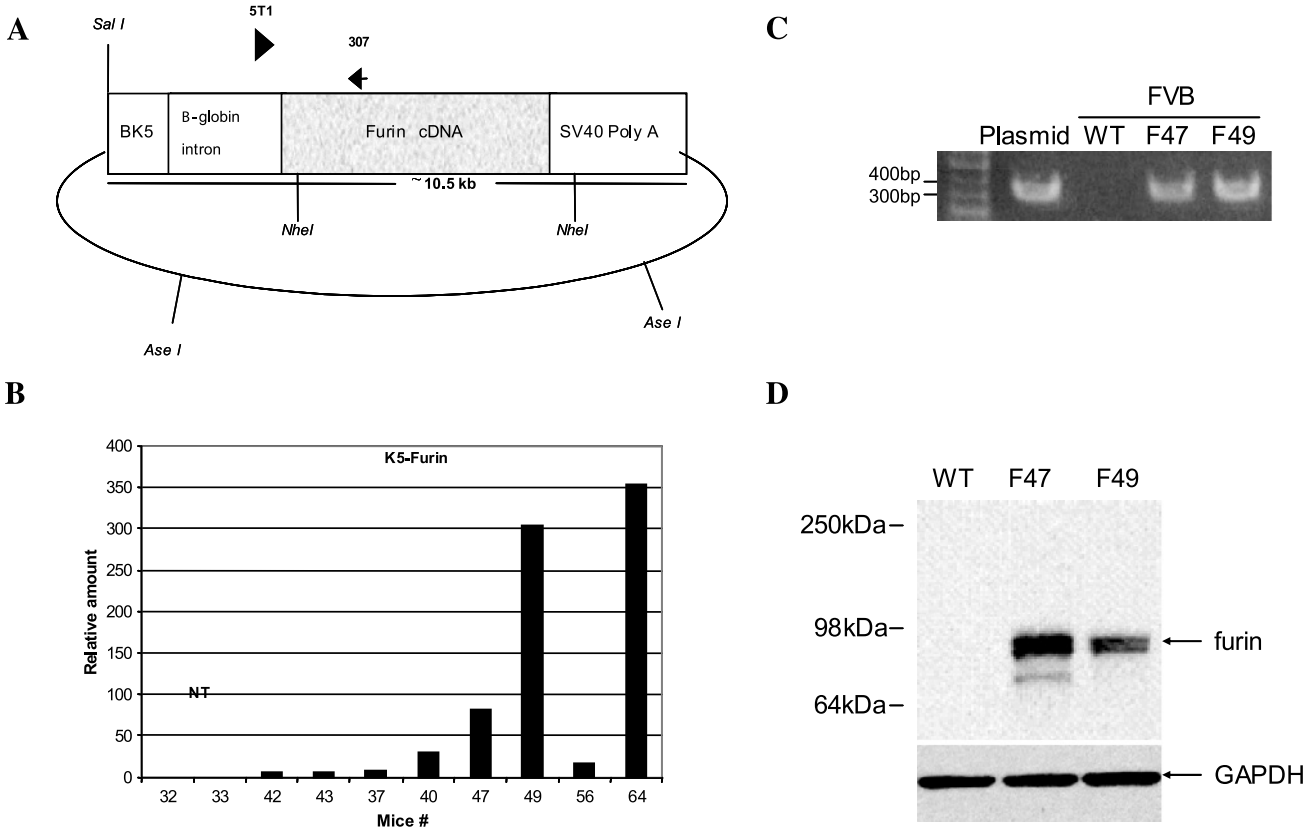

Figure 1. Generation of furin transgenic mice. (A) K5-Furin construct. (B) Real-time PCR quantification of the transgene present in several founders. (C) PCR from DNA extracted from mouse tails, showing WT and two different animal founders that were used for most experiments. (D) Western blot showing differential expression of furin protein in transgenic lines. Note the complete absence of furin expression in the WT mice.

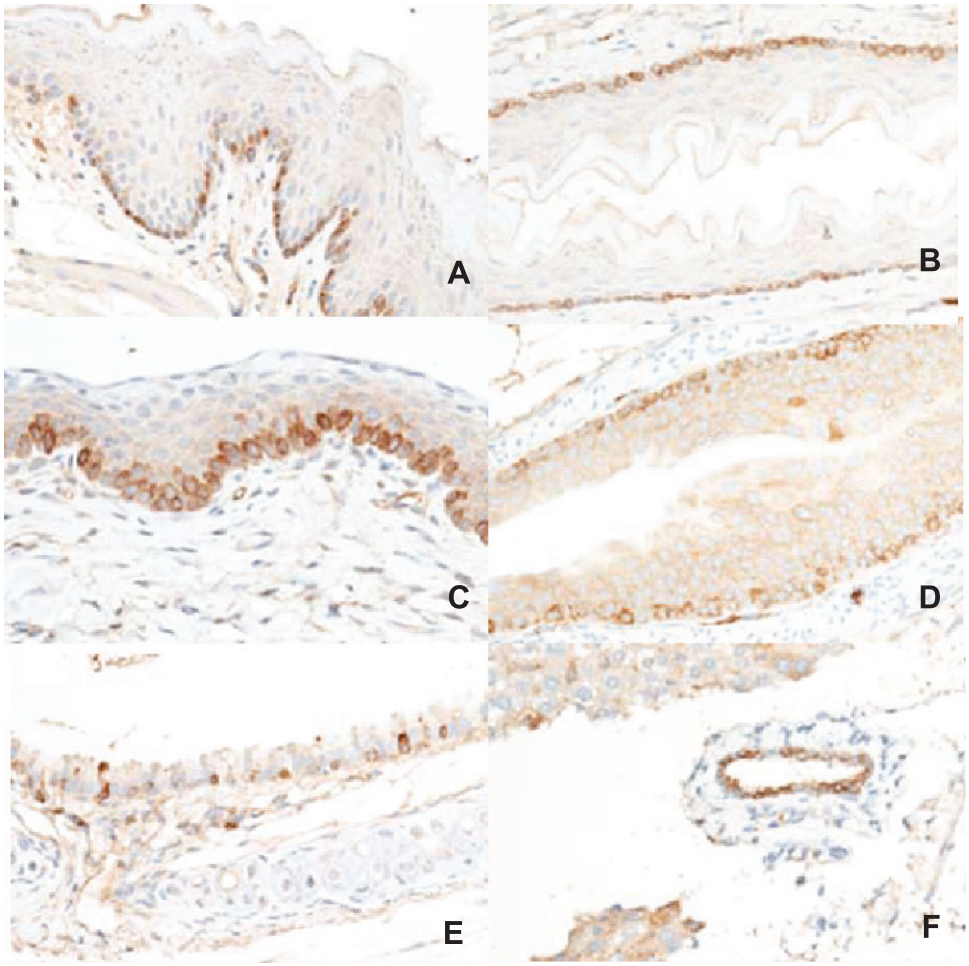

Figure 2. Immunhistochemical detection of furin expression in the basal layer of several epithelia of transgenic mice. Tail epidermis (A), esophageal epithelium (B), oral epithelium (C), urothelium of the ureter (D), bronchial epithelium showing positive immunostain in several basal cells (E), and biliary duct epithelium (F). Tissues are from the F47 mouse line. Immunohistochemistry and hematoxylin counterstain, ×100.

(MON-148, ALX-803-015; ALEXIS) was used as a primary antibody at 1:200. An avidin-biotin-peroxidase kit (Vectastain Elite; Vector) was then used followed by the chromogen 3′, 3′-diaminobenzidine to develop the immunostain. Negative controls were incubated in the absence of the primary antibody with serum at the same protein concentration as the primary antibody. All sections were counterstained with hematoxylin and mounted. Furin-positive cells were counted in the interfollicular epidermis and expressed as furin-positive cells per millimeter of epidermal BM. Basement membrane length was determined in furin-stained skin sections, and the furin-positive cells of the respective interfollicular epidermal sector was counted using a morphometry software that permits length measurements of digitalized images (Image Pro-Plus; Media Cybernetics). BM length was determined in acetone- (control) and TPA-treated epidermis (three to five mice per group; minimum BM length/mouse was 2 mm per section).

Gene Expression Analysis by Real-time PCR

RNA was extracted using the RNAqueous kit from Ambion (Austin, TX). Quality was assessed using a RNA 6000 Nano LabChip on an Agilent 2100 BioAnalyzer. Contaminating DNA from RNA preparations was removed using TURBO DNA-free (Ambion). RNA was quantified using a Nanodrop (Nanodrop Technologies, Wilmington, DE). RNA was reverse-transcribed (RT) using the M-MLV reverse transcriptase (Ambion) and a mixture of anchored oligodT and random decamers. For each sample, two RT reactions were performed with 100 and 25 ng of total RNA, respectively. Aliquots of cDNA were used for quantitative PCR. Real-time PCRs were performed in duplicates using an Applied Biosystems (Foster City, CA) 7900 HT instrument and Applied Biosystems master mix. A 5-point, four-fold standard curve was constructed from serial dilution with one of the samples to confirm linearity of the RT step, PCR efficiency was close to 2, and to convert the cycle threshold values into quantities. Cycling conditions were 95°C, 15 min, followed by 40 (two steps) cycles (95°C for 15 seconds and 60°C for 60 seconds). The primers for human furin were as follows: forward, GAGATTGAAAACACCAGCGAA; reverse, GCGGTGCCATAGAGTACGAG; probe, 6fam-AACAACTATGGGACGCTGACCAAGTTCAC-bhq1. For mouse furin, the primers were as follows: forward, TCCTAGAGATTGAAAATACCAGTGAAG; reverse, GGCTGTGCCATACAGAACGA; probe, 6fam-AACAACTATGGGACGCTGACCAAGTTCAC-bhq1. For mouse PACE4, the primers were as follows: forward, AACCTCCTGCATCACCAACC; reverse, AGCCGATTGGACTTCACCAT; probe, 6fam-ACGTGCAGCAATGCCGATGAGACT-bhq1. For mouse PC5, the primers were as follows: forward, CTGATGGATGCCGAAGCC; reverse,

CTGTTTGGTCGAATGGTCTTGA (this was a SYBR Green assay, whereas the others were TaqMan assays).

The following mouse primers were obtained from Applied Biosystems: Mm00478295_m1 for ppib, Mm00479023_m1 for PC1/3, Mm00500981_m1 for PC2, Mm00801899_m1 for PC4, and Mm00476621_m1 for PC7.

Statistical Analysis

Both two-sample *t* test and Wilcoxon tests were used to compare tumor incidence and tumor volume. Wilcoxon test, a nonparametric test, was used when sample size was small. The *t* test was used when the sample size in each comparison group was greater than 30. $P < .05$ was considered statistically significant. All statistical analyses were performed using SAS 9.2 (SAS Institute Inc, Cary, NC).

Results

Generation and Characterization of Transgenic Mice

To study the effects of furin expression on the highly proliferative epidermal basal cells, we subcloned the full-length human furin cDNA into an expression vector containing bovine K5 promoter, which can

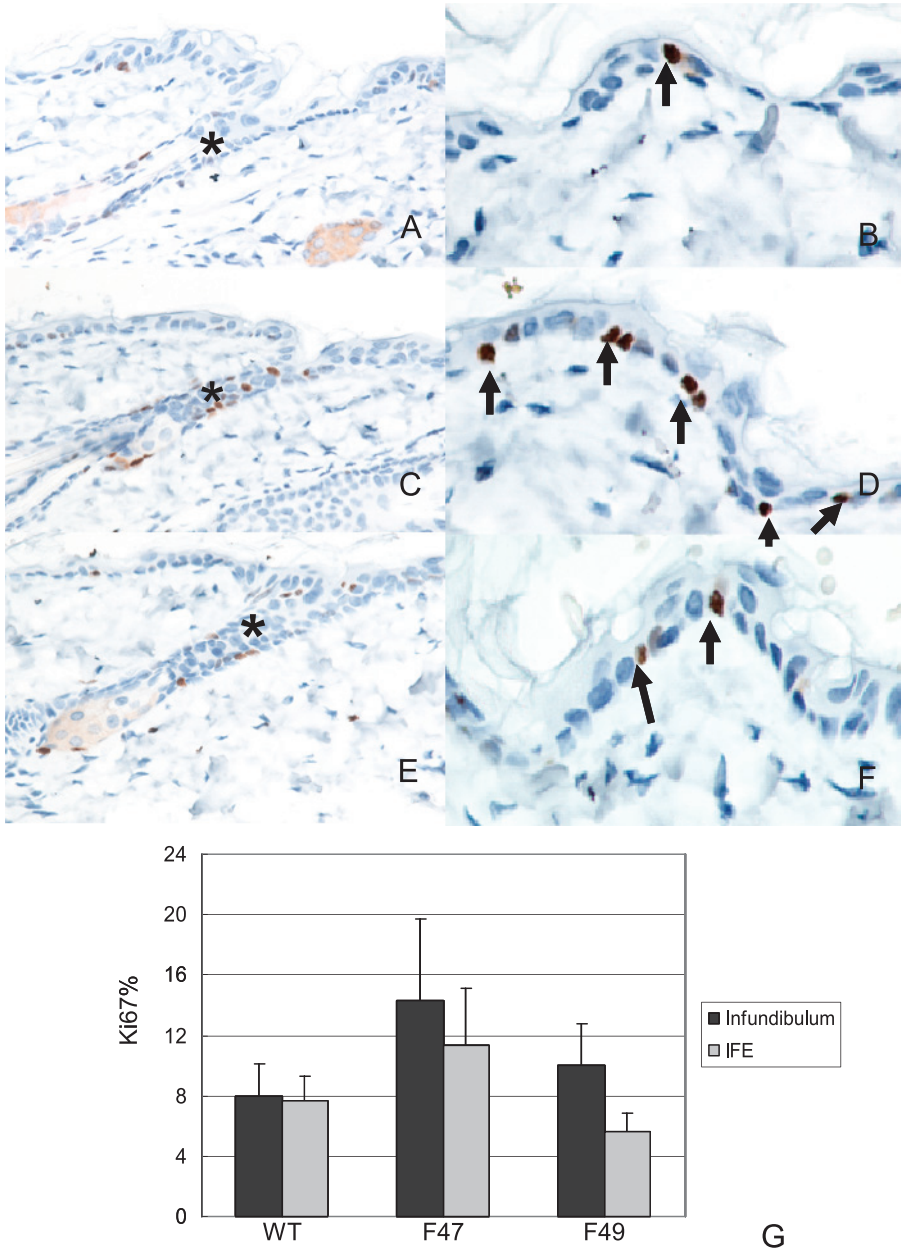

Figure 3. Ki67 detection in normal (untreated) mouse dorsal epidermis. A (WT), C (F47), and E (F49) show lower magnification images (×100) of a sector of skin centered on a hair follicle showing the infundibulum or intrafollicular epidermis (*). B (WT), D (F47), and F (F49) show at a higher magnification the interfollicular epidermis (×200). Note that the animal line F47 (C and D) exhibit more Ki67-positive cells than the other two animal groups. (G) Quantification of Ki67-positive cells expressed as percentage of Ki67-positive basal keratinocytes in the infundibulum and in the interfollicular epidermis (IFE). Ki67 immunohistochemistry and hematoxylin counterstain.

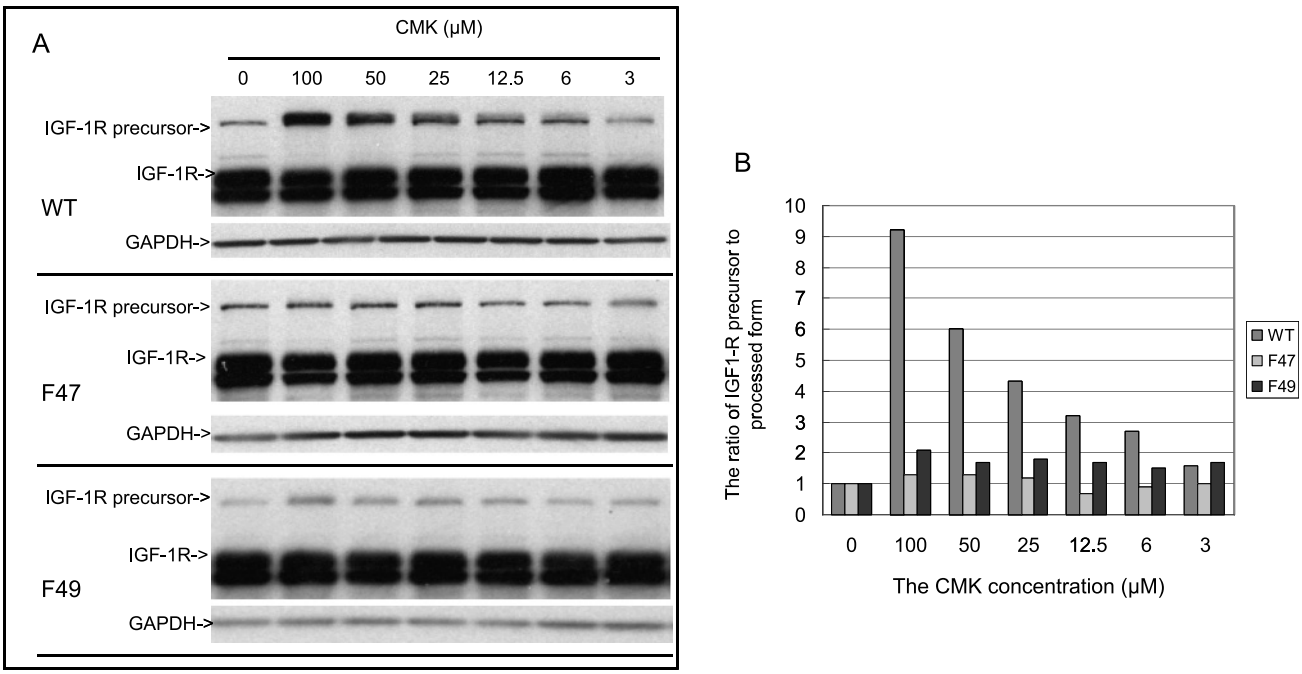

Figure 4. (A) Western blot analysis of IGF-1R processing in WT and transgenic primary keratinocyte cultures. The cells were challenged *in vitro* with different doses of the PC inhibitor CMK to investigate the sensitivity of primary keratinocytes to IGF-1R cleavage inhibition by CMK. A dose of 6 μM CMK was able to inhibit PC-mediated IGF-1R processing in WT keratinocytes, and the inhibitory effect was directly proportional to the CMK dose up to 100 μM. The effect was noted by the increasing presence of IGF-1R precursor or proform with increasing concentrations of CMK. Conversely, the CMK treatment failed to increase significantly the levels of the IGF-1R precursor in F47- and F49-derived cells. (B) Changes as depicted by plotting the ratios of densitometric evaluations of IGF-1R precursor to processed bands.

direct furin expression to the basal skin keratinocytes. The construct (Figure 1*A*) contains the bovine K5 promoter, followed by the first intron of the rabbit β-globin gene to enhance the efficiency of transcription, the full-length furin cDNA, and, finally, the polyadenylation signal from SV-40. A number of founders were produced, and mouse tail DNA samples were used to determine the relative transgene dosage using real-time PCR analysis. As shown in Figure 1*B*, lines 47, 49, and 64 demonstrated relatively higher copy number of the furin transgene as determined by real-time PCR. Because the transgene could only be detected in the male progeny of line 64 and we only use female mice for skin carcinogenesis experiments, lines 47 and 49 (called F47 and F49) were used for all the following experiments. The two transgenic lines were genotyped by PCR of genomic DNA using the primers amplifying a DNA segment between 300 and 400 bp and a representative genotyping experiment is shown in Figure 1*C*. Transgene expression was confirmed by Western blot analysis of furin protein expression. Furin protein was clearly expressed in the keratinocytes from both transgenic mouse lines (molecular weight ~100 kDa). WT keratinocytes showed no or minimal furin expression (Figure 1*D*). Densitometric evaluation of four different Western blots demonstrated that line F47-derived epidermal keratinocytes expressed almost twice as much furin as line F49-derived keratinocytes (ratio F47/F49 = 1.82 ± 0.44).

Effect of Furin Expression in the Epidermis

The distribution of furin expression in transgenic mice was further analyzed by immunohistochemical (IHC) staining. In WT mouse, furin expression was not seen; although occasionally, it could be observed as minimal punctuate staining in the perinuclear cytoplasm of basal epithelial cells in the epidermis and squamous mucosae (not shown). Conversely, furin was clearly detected by IHC in most squamous epithelia of transgenic mice (Figure 2). The location of furin was cytoplasmic, predominately overexpressed in the epidermal basal layer in both transgenic lines (Figure 2*A*). The cytoplasmic perinuclear staining pattern of furin is in accordance with its known Golgi and *trans*-Golgi network localization. In addition, the furin staining was detected in the epithelial basal layer of the oral mucosa, esophagus, exocervix, ureter, bronchus, and the epithelial cells of biliary ducts in transgenic mice (Figure 2, *B-F*).

No gross phenotypic alterations were observed by the expression of furin in transgenic mouse lines. Nevertheless, differences in cell proliferation were detected in the transgenic epidermis when compared with WT. The percent of Ki67-positive basal keratinocytes in the infundibular (intrafollicular) epidermis was almost twice as high in F47 compared with WT mice ($P < .001$) and approximately 20% higher in F49 than in WT mice ($P < .06$). In the interfollicular epidermis only the F47 basal keratinocyte Ki67 index was significantly higher than in WT mice ($P < .005$) (Figure 3).

IGF-1R, one of the major substrates of furin, may be responsible of the proproliferative effects of furin [8]. Thus, we examined the processing of IGF-1R in mouse-derived epidermal primary keratinocyte cultures. Interestingly, the difference of IGF-1R processing in keratinocytes derived from WT and F47 and F49 mice was marginal, suggesting that the endogenous furin expressed in WT keratinocytes efficiently processed pro IGF-1R. To observe a difference in the activating ability of transgenic and WT derived keratinocytes, we

challenged the cells *in vitro* with different doses of the PC inhibitor CMK to investigate the sensitivity of primary keratinocytes to IGF-1R cleavage inhibition by CMK. As shown in Figure 4, a dose as low as 6 μM CMK was able to inhibit PC-mediated IGF-1R processing in WT keratinocytes, and the inhibitory effect was directly proportional to the CMK dose up to a maximal effect at a dose of 100 μM CMK that displayed the maximal effect. The effect was noted by the increasing presence of IGF-1R proform with increasing concentrations of CMK (Figure 4). Conversely, the CMK treatment, even at the highest dose, failed to increase the levels of the IGF-1R proform in F47 and F49-derived cells, suggesting that the high overexpression of furin in transgenic mouse keratinocytes overcomes the inhibitor and the PC is able to activate the IGF-1R substrate leaving little proform behind.

Short-term In Vivo *Experiments*

To evaluate differences in epidermal proliferation between WT and transgenic mouse, we treated the skin topically with two doses of TPA (separated by 48 hours) and analyzed furin expression and Ki67 index by IHC 48 hours after the last TPA administration. Interestingly, furin expression in F47 and F49 mouse epidermis was significantly enhanced by the phorbol ester treatment ($P < .001$; Figure 5). Both F47 and F49 epidermis showed an increase in the number of furin-expressing keratinocytes after TPA application. This expression was more intense in F47 than in F49 mice, whereas the number of positively stained basal keratinocytes was similar in both lines. In addition, line F47 exhibited a much larger number of parabasal keratinocytes that expressed this PC, and the intensity was also higher in this layer (Figure 5). As expected, the tumor promoter TPA dramatically stimulated

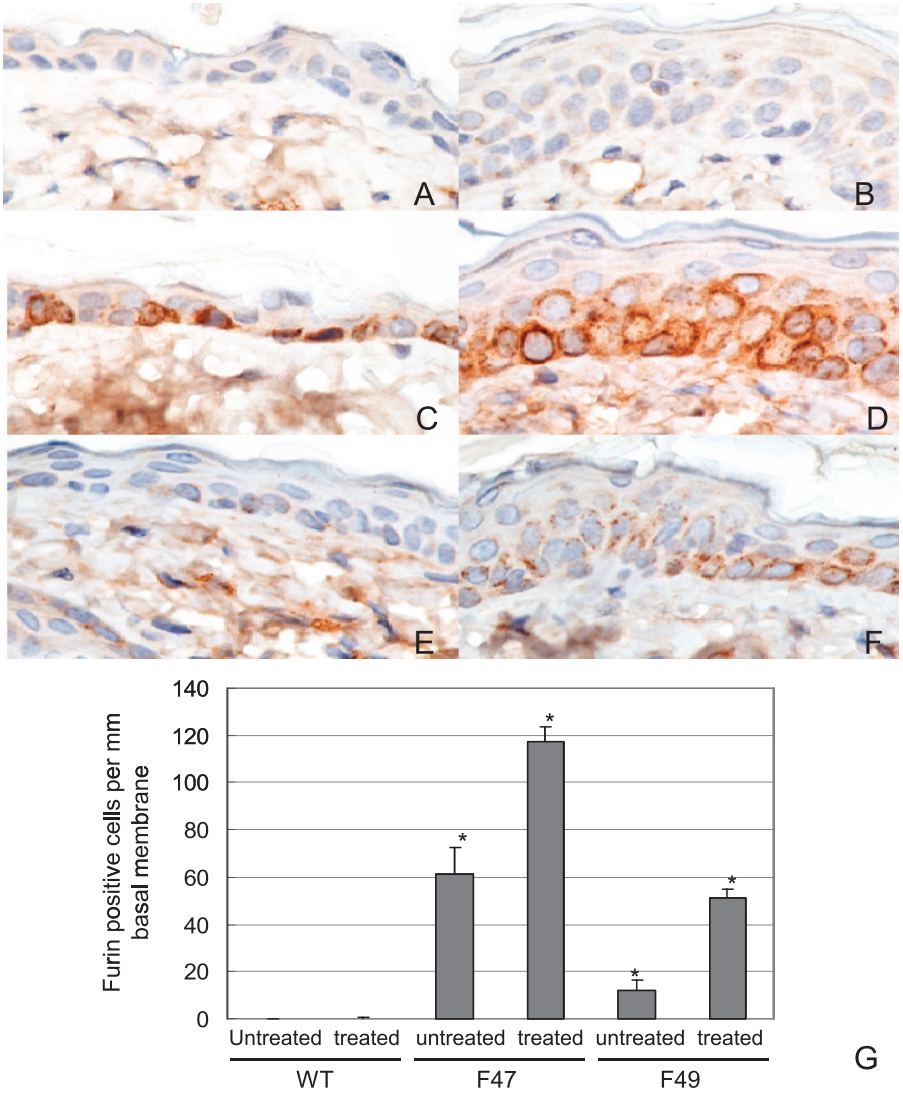

Figure 5. Immunohistochemistry of furin in dorsal mouse epidermis. A (WT), C (F47), and E (F49) depict acetone control epidermis. C (F47) contains numerous furin-positive basal keratinocytes that are not obvious in the two other animal groups. B (WT), D (F47), and F (F49) show epidermis treated with the phorbol ester (TPA). Although the untreated WT epidermis has negative (A), the TPA-treated WT epidermis showed occasional moderate to marginal endogenous furin expression in the perinuclear area of some parabasal keratinocytes (B and inset). Untreated epidermis from F47 exhibits a large increase in furin-positive basal cells (C) that further increased together with positive parabasal keratinocytes after TPA treatment (D). Epidermis from F49 also shows expression of furin in basal keratinocytes, but as seen in the histogram (G), this increase is markedly smaller than the one detected in F47 mice. Asterisks indicate significantly different changes when compared with the respective WT.

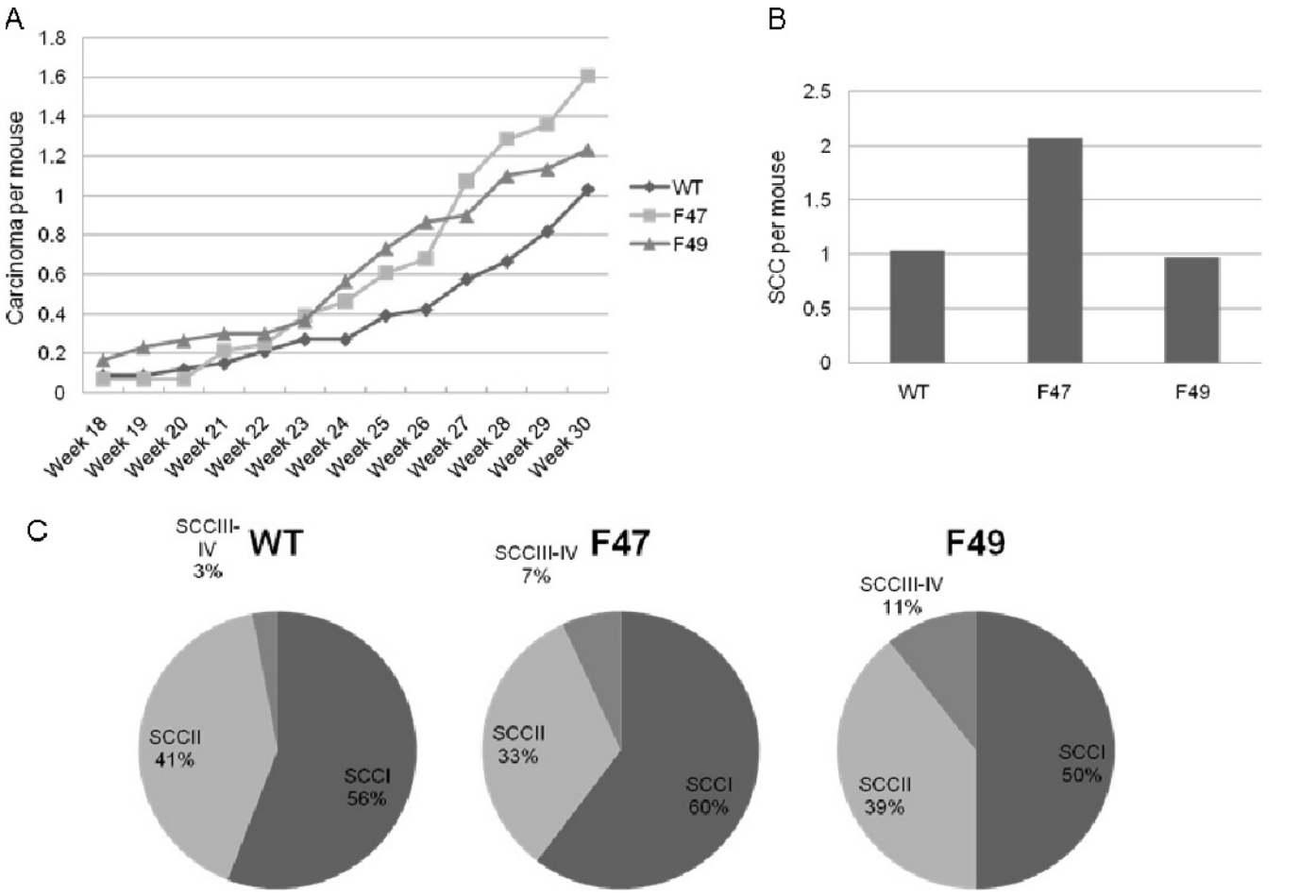

Figure 6. Results of skin chemical carcinogenesis experiments. (A) Prevalence of tumor multiplicity as expressed by SCC/mouse during the course of the experiment as counted weekly and determined by the presence of large (>10 mm) infiltrating or ulcerated lesions of the dorsal skin. (B) The number of SCC/mouse at the last time point (30 weeks) as determined by histopathologic analysis. (C) The pie charts reflect the percentage of each type of SCC at the 30th week following the grading scale described in Materials and Methods.

the keratinocyte proliferation in the skin samples from all groups, approximately three- to four-fold compared with sham treated control epidermis (not shown). Nevertheless, the increased proliferation rates after TPA treatment were similar in WT and transgenic mice.

Skin Carcinogenesis Experiments

To investigate the role of furin during carcinogenesis, we treated WT and transgenic animals using a two-stage carcinogenesis protocol. Skin papillomas and carcinomas developed in both transgenic and WT groups at approximately 11 and 18 weeks, respectively, suggesting that furin drives a premature increased proliferation, leading to early tumor development. More papillomas were noted in F47 and F49 mice than in the WT animal group. Conversely, the prevalence of SCCs was similar in these two groups until week 23, and it was in the last 7 weeks (week 23 to week 30) that the number of SCC/mouse was higher in the transgenic lines than in WT mice (Figure 6*A*), pointing to a furin-dependent acceleration in both early development and conversion rates. Thus, both transgenic lines, especially F47, developed a higher number of SCCs than WT in almost each point recorded. The incidence of malignant tumors in F47 mice, that is, the percentage of mice with carcinomas, was consistently higher than in WT mice. The tumor incidence of F49 and WT mice was similar. The mean number of carcinomas per mouse at week 30 was approximately 1.00, 1.23, and 1.61 ($P < .05$) for WT, F49, and F47 mice, respectively. Histologic diagnosis obtained at week 30 (histogram in Figure 6*B*) showed that the SCC multiplicity of F47 (2.07 SCC/mouse; *vs* the gross count of 1.61 seen in Figure 6*A*) was double that of WT (1.03 SCC/mouse; $P < .002$), whereas the increased carcinoma/mouse observed in F49 mice was not statistically significant. Interestingly, although most SCC produced by the two-stage carcinogenesis protocol were low-grade tumors, the percentage of high-grade SCC (SCC grades 3 and 4) was 7% and 11% of total SCC in the F47 and F49 groups, respectively, compared with 3% for WT mice (pie charts in Figure 6*C*). Tumor volume in transgenic mice was consistently higher than that in WT mice, especially in F49 mice, for example, at 30 weeks, the mean volume of tumors was 190 ± 35 mm^3 in WT mice *versus* 390 ± 121 mm^3 in the transgenic mice ($P < .04$). In line F47, the mean volume was 310 ± 188 mm^3 at 30 weeks, but because of the dispersion of values, it did not reach statistical significance (*t* test).

We were also able to detect processing of furin substrates in tumor lysates obtained from WT and transgenic mice. As shown in Figure 7, the transgenic SCC cells, by and large, were able to process more efficiently the precursors of IGF-IR and TGF-β than the WT-derived tumor cells.

Expression of Other PCs after Transgenic Furin Expression

To evaluate the possible effect of forced transgene expression on other PCs in epidermal cells, we evaluated the expression of PC RNA using quantitative real-time PCR. As seen in Figure 8*A*, the transgene (hFur) was expressed in normal murine keratinocytes derived from animal lines F47 and F49 and naturally absent in WT keratinocytes. The levels of expression in F47 keratinocytes was three-fold higher than those in F49 cells, thus showing a similar trend as the protein expression detected by Western blot analysis (Figure 1*D*). PC1 and PC4 were undetectable in WT, F47, and F49 keratinocytes. In addition, the cultured normal keratinocytes from the three different animal groups did not show major differences in PC transcript expression levels. One exception is the relatively high levels of PC2 in the transgenic keratinocytes. The difference with WT expression is significant and could be due to longer Merkel cell survival in the transgenic cell cultures. Expression of PC RNAs in SCCs derived from carcinogen-treated mice showed a similar trend with undetectable PC1, PC2, and PC4, whereas the other PCs showed little or no change when comparing WT to transgenic tumors.

Discussion

Furin is a serine protease that is frequently overexpressed in several human cancer cell lines and malignancies [24,26,27,36,42,43] including several murine cell lines derived from skin tumors induced by chemical carcinogenesis [44]. Its activity results in proteolytic cleavage of substrates leading to activation of many cancer-related proteins including important growth factors and receptors such as IGF-1 and its receptor IGF-1R, TGF-β, etc. [8,30,45–47].

To evaluate the *in vivo* effects of furin on skin biology and tumorigenesis, we developed two K5-Furin mouse lines (F47 and F49). Real-time PCR and Western analyses showed that F47 mice expressed approximately twice as much furin as F49 mice at the protein level. IHC analysis of both lines revealed increased number of basal keratinocytes expressing furin. The enhanced furin expression was reflected in higher levels of activated IGF-1R as demonstrated by Western blot analysis. This increase was more obvious and significant in F47 than in F49 mice. Similarly, the basal keratinocyte proliferation rate of the epidermis in F47 mice was significantly elevated over the WT and F49 counterparts. Interestingly, this difference was more prominent and significant in the infundibulum or intrafollicular segment of the epidermis than in the interfollicular epidermis. This difference is even more noteworthy if one takes into account several reports pointing to the hair follicle and, in particular, to the suprasebaceous component of this epidermal appendix as the origin of nonmelanoma skin neoplasia [48–50].

In a previous report, we found that another PC, PACE4, had a pivotal role in enhancing mouse skin tumor development and invasion [35]. Because PACE4 is localized extracellularly, it has easy access to intercellular and matrix-associated substrates such as metalloproteases and is able to enhance tumor cell invasion. Furin, however, might have a more prominent role in activating intracellular cancer–related substrates that may influence other cellular processes such as proliferation. This possible divergence in function is supported by our results showing that keratinocytes derived from untreated transgenic mice expressing furin in the epidermal basal layer as well as tumor cells derived from transgenic animals were able to process IGF-1R and TGF-β. As a consequence of increased growth factor processing, transgenic

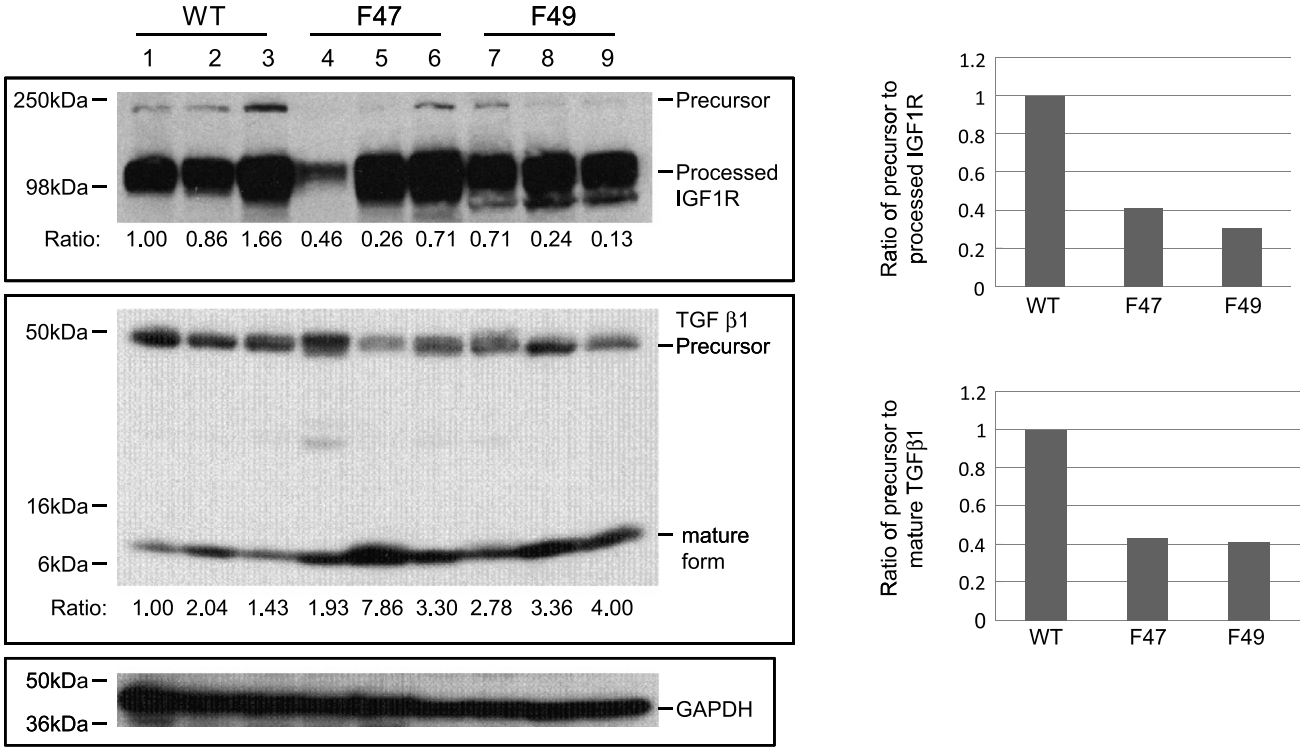

Figure 7. Western blot analysis of mouse tumor lysates obtained at the 30th week. Processing of IGF-1R and TGF-β shows an increased ability of SCC cells from K5-Furin mice to process these two furin substrates compared with a lower activation and larger accumulation of the precursor or proform in WT tumor cells. Histograms show these changes as detected by densitometric quantification.

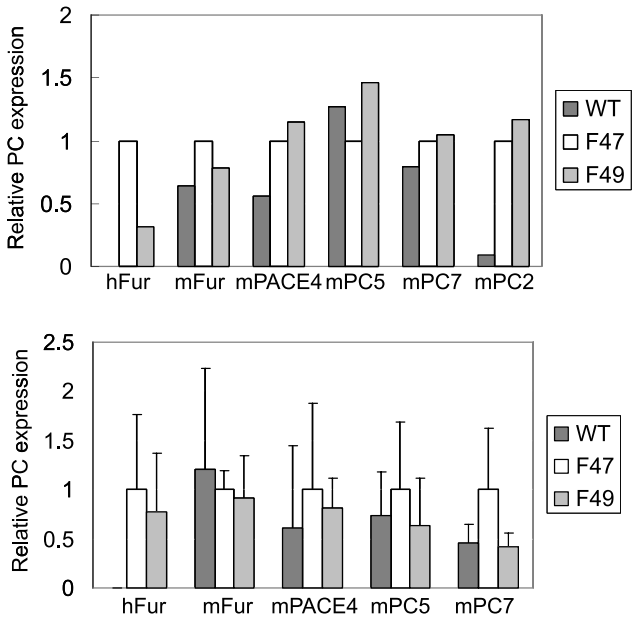

Figure 8. Quantitative real-time PCR of PCs using either mouse normal keratinocytes in short-term culture (A) or mouse SCC tissues obtained after treatment with a two stage carcinogenesis protocol (three tumors per group; bar indicates mean ± SD; B). All PC transcript expression values (in the *y* axis) were normalized to the internal control peptidylpropyl isomerase B and then expressed relative to F47. PC1 and PC4 expression was undetectable in mouse keratinocytes and tumors, and PC2 was undetectable in tumors. Except for furin, where both human (transgenic) (hFur) and endogenous murine furin (mFur) were evaluated, the rest of the PCs detected were endogenous mouse PCs.

epidermis showed a higher proliferative rate than control WT epidermal cells *in vivo*. Conversely, we were unable to detect differences in processing of MT1-MMP and MT2-MMP in WT and transgenic epidermal cells derived from the two animal lines F47 and F49 (not shown). In a previous report [35], we demonstrated that K5-PACE4 keratinocytes were able to process membrane-type MMPs and have an increased invasive ability, suggesting that furin and PACE4 may exert different functions, despite their similar enzyme properties.

To demonstrate a causal relationship between furin expression and increased tumorigenesis *in vivo*, we studied furin-overexpressing transgenic and WT mice treated with a two-stage skin carcinogenesis protocol. During the entire experimental period after the appearance of benign tumors or papillomas, the mean number of papillomas/mouse was higher in both transgenic mouse lines than in WT mice. More importantly, the mean number of SCC/mouse showed a similar tendency, in both lines at 30 weeks of treatment with the two-stage carcinogenesis protocol; the number of carcinomas per animal was higher than in WT mice, although this difference was most marked in F47 mice. Moreover, the incidence of malignant tumors, which is defined as the percentage of animals harboring carcinomas, was consistently higher in transgenic mice. In addition, tumor multiplicity and tumor volume were remarkably higher in transgenic mice when compared with WT mice, probably reflecting the increased proliferative rate evidenced in short-term *in vivo* experiments as well as by the increased processing of IGF-1R and TGF-β seen in carcinomas derived from transgenic mice.

Metastases in axial lymph nodes and lung were also higher in number in transgenic mice than in WT mice. Because of the low numbers of animals bearing metastases (mice had to be euthanized at 30 weeks because of the large and numerous skin primary tumors), the results were not statistically significant.

To assess a possible interference of the transgenic expression of furin in epidermal keratinocytes, we conducted an evaluation of the RNA expression of six other PCs in normal keratinocytes and SCCs derived from WT, F47, and F49 mice. The quantitative real-time PCR results showed that enforced furin expression had no or had minimal effect on the levels of PACE4, PC5, and PC7, whereas PC1 and PC4 were undetectable in both normal keratinocytes and SCC cells. PC2 was detected at higher levels in transgenic keratinocytes than in their WT counterparts. This effect may be due to a higher number or an enhanced survival of Merkel cells in the short-term cultures of transgenic epidermal cells. Merkel cells are known to express high levels of PC2 [51]. Because this difference was not seen in the tumor cells where PC2 was undetectable in WT, F47, and F49 SCCs, it is doubtful that transgenic furin could have an enhancing effect on PC2 transcript expression during tumor development.

The data indicate that increased furin expression enhanced tumor development and growth without significantly affecting the expression of other endogenous PCs. It is noteworthy that the higher prevalence of SCCs in the transgenic line F47 *versus* line F49 correlated well with the relatively higher expression of furin in basal keratinocytes of line F47 as well with its increased baseline keratinocyte proliferation rate and also with a higher expression of furin in the SCCs of line F47 when compared with their counterparts in line F49, suggesting that there might be a dose-response type effect between the transgene level of expression and the susceptibility to skin chemical carcinogenesis.

Taken together, furin expression targeted *in vivo* to the epidermis resulted in increased epidermal proliferation as well as increased cancer-related substrate activation that had a protumorigenic effect that was demonstrated by an increased susceptibility to carcinogen-induced skin tumors as exemplified by an enhanced SCC multiplicity and tumor volume. Because furin expression and activity are enhanced in lung and head and neck cancers [24,26,27,36,42,43], these experimental data further support the possible use of furin as a target in human cancer treatment.

Acknowledgments

The authors thank the following core facilities at Fox Chase Cancer Center for their help: the Histopathology Facility, the Transgenic Mouse Facility, the Laboratory Animal Facility, the Genomics Facility, and the Biostatistics and Bioinformatics Facility.

References

[1] Seidah NG (2011). What lies ahead for the proprotein convertases? *Ann N Y Acad Sci* **1220**, 149–161.

[2] Seidah NG (2011). The proprotein convertases, 20 years later. *Methods Mol Biol* **768**, 23–57.

[3] Molloy SS, Anderson ED, Jean F, and Thomas G (1999). Bi-cycling the furin pathway: from TGN localization to pathogen activation and embryogenesis. *Trends Cell Biol* **9**, 28–35.

[4] Seidah NG, Benjannet S, Wickham L, Marcinkiewicz J, Jasmin SB, Stifani S, Basak A, Prat A, and Chretien M (2003). The secretory proprotein convertase neural apoptosis–regulated convertase 1 (NARC-1): liver regeneration and neuronal differentiation. *Proc Natl Acad Sci USA* **100**, 928–933.

[5] Seidah NG, Mowla SJ, Hamelin J, Mamarbachi AM, Benjannet S, Toure BB, Basak A, Munzer JS, Marcinkiewicz J, Zhong M, et al. (1999). Mammalian

subtilisin/kexin isozyme SKI-1: a widely expressed proprotein convertase with a unique cleavage specificity and cellular localization. *Proc Natl Acad Sci USA* **96**, 1321–1326.

[6] Duguay SJ, Milewski WM, Young BD, Nakayama K, and Steiner DF (1997). Processing of wild-type and mutant proinsulin-like growth factor-IA by subtilisin-related proprotein convertases. *J Biol Chem* **272**, 6663–6670.

[7] Lehmann M, Andre F, Bellan C, Remacle-Bonnet M, Garrouste F, Parat F, Lissitsky JC, Marvaldi J, and Pommier G (1998). Deficient processing and activity of type I insulin-like growth factor receptor in the furin-deficient LoVo-C5 cells. *Endocrinology* **139**, 3763–3771.

[8] Khatib AM, Siegfried G, Prat A, Luis J, Chretien M, Metrakos P, and Seidah NG (2001). Inhibition of proprotein convertases is associated with loss of growth and tumorigenicity of HT-29 human colon carcinoma cells: importance of insulin-like growth factor-1 (IGF-1) receptor processing in IGF-1–mediated functions. *J Biol Chem* **276**, 30686–30693.

[9] Stawowy P, Meyborg H, Stibenz D, Borges Pereira Stawowy N, Roser M, Thanabalasingam U, Veinot JP, Chretien M, Seidah NG, Fleck E, et al. (2005). Furin-like proprotein convertases are central regulators of the membrane type matrix metalloproteinase–pro–matrix metalloproteinase-2 proteolytic cascade in atherosclerosis. *Circulation* **111**, 2820–2827.

[10] Cao J, Rehemtulla A, Pavlaki M, Kozarekar P, and Chiarelli C (2005). Furin directly cleaves proMMP-2 in the *trans*-Golgi network resulting in a nonfunctioning proteinase. *J Biol Chem* **280**, 10974–10980.

[11] Wang P, Tortorella M, England K, Malfait AM, Thomas G, Arner EC, and Pei D (2004). Proprotein convertase furin interacts with and cleaves pro-ADAMTS4 (Aggrecanase-1) in the *trans*-Golgi network. *J Biol Chem* **279**, 15434–15440.

[12] Komiyama T, Coppola JM, Larsen MJ, Van Dort ME, Ross BD, Day R, Rehemtulla A, and Fuller RS (2009). Inhibition of furin/proprotein convertase–catalyzed surface and intracellular processing by small molecules. *J Biol Chem* **284**, 15729–15738.

[13] Yana I and Weiss SJ (2000). Regulation of membrane type-1 matrix metalloproteinase activation by proprotein convertases. *Mol Biol Cell* **11**, 2387–2401.

[14] Bergeron E, Basak A, Decroly E, and Seidah NG (2003). Processing of α_4 integrin by the proprotein convertases: histidine at position P6 regulates cleavage. *Biochem J* **373**, 475–484.

[15] Mayer G, Boileau G, and Bendayan M (2003). Furin interacts with proMT1-MMP and integrin α_V at specialized domains of renal cell plasma membrane. *J Cell Sci* **116**, 1763–1773.

[16] Smirnov SP, Mcdearmon EL, Li S, Ervasti JM, Tryggvason K, and Yurchenco PD (2002). Contributions of the LG modules and furin processing to laminin-2 functions. *J Biol Chem* **277**, 18928–18937.

[17] Lissitzky JC, Luis J, Munzer JS, Benjannet S, Parat F, Chretien M, Marvaldi J, and Seidah NG (2000). Endoproteolytic processing of integrin pro-α subunits involves the redundant function of furin and proprotein convertase (PC) 5A, but not paired basic amino acid converting enzyme (PACE) 4, PC5B or PC7. *Biochem J* **346**(pt 1), 133–138.

[18] Lehmann M, Rigot V, Seidah NG, Marvaldi J, and Lissitzky JC (1996). Lack of integrin α-chain endoproteolytic cleavage in furin-deficient human colon adenocarcinoma cells LoVo. *Biochem J* **317**(pt 3), 803–809.

[19] Khatib AM, Siegfried G, Chretien M, Metrakos P, and Seidah NG (2002). Proprotein convertases in tumor progression and malignancy: novel targets in cancer therapy. *Am J Pathol* **160**, 1921–1935.

[20] De Cicco RL, Bassi DE, Benavides F, Conti CJ, and Klein-Szanto AJ (2007). Inhibition of proprotein convertases: approaches to block squamous carcinoma development and progression. *Mol Carcinog* **46**, 654–659.

[21] Artenstein AW and Opal SM (2011). Proprotein convertases in health and disease. *N Engl J Med* **365**, 2507–2518.

[22] D'anjou F, Routhier S, Perreault JP, Latil A, Bonnel D, Fournier I, Salzet M, and Day R (2011). Molecular validation of PACE4 as a target in prostate cancer. *Transl Oncol* **4**, 157–172.

[23] Schalken JA, Roebroek AJ, Oomen PP, Wagenaar SS, Debruyne FM, Bloemers HP, and Van De Ven WJ (1987). *fur* gene expression as a discriminating marker for small cell and nonsmall cell lung carcinomas. *J Clin Invest* **80**, 1545–1549.

[24] Mbikay M, Sirois F, Yao J, Seidah NG, and Chretien M (1997). Comparative analysis of expression of the proprotein convertases furin, PACE4, PC1 and PC2 in human lung tumours. *Br J Cancer* **75**, 1509–1514.

[25] Bassi DE, Lopez De Cicco R, Mahloogi H, Zucker S, Thomas G, and Klein-Szanto AJ (2001). Furin inhibition results in absent or decreased invasiveness and tumorigenicity of human cancer cells. *Proc Natl Acad Sci USA* **98**, 10326–10331.

[26] Bassi DE, Mahloogi H, Al-Saleem L, Lopez De Cicco R, Ridge JA, and Klein-Szanto AJ (2001). Elevated furin expression in aggressive human head and neck tumors and tumor cell lines. *Mol Carcinog* **31**, 224–232.

[27] Bassi DE, Mahloogi H, Lopez De Cicco R, and Klein-Szanto A (2003). Increased furin activity enhances the malignant phenotype of human head and neck cancer cells. *Am J Pathol* **162**, 439–447.

[28] Lopez De Cicco R, Bassi DE, Zucker S, Seidah NG, and Klein-Szanto AJ (2005). Human carcinoma cell growth and invasiveness is impaired by the propeptide of the ubiquitous proprotein convertase furin. *Cancer Res* **65**, 4162–4171.

[29] Siegfried G, Khatib AM, Benjannet S, Chretien M, and Seidah NG (2003). The proteolytic processing of pro–platelet-derived growth factor-A at RRKR(86) by members of the proprotein convertase family is functionally correlated to platelet-derived growth factor-A–induced functions and tumorigenicity. *Cancer Res* **63**, 1458–1463.

[30] Siegfried G, Basak A, Cromlish JA, Benjannet S, Marcinkiewicz J, Chretien M, Seidah NG, and Khatib AM (2003). The secretory proprotein convertases furin, PC5, and PC7 activate VEGF-C to induce tumorigenesis. *J Clin Invest* **111**, 1723–1732.

[31] Scamuffa N, Siegfried G, Bontemps Y, Ma L, Basak A, Cherel G, Calvo F, Seidah NG, and Khatib AM (2008). Selective inhibition of proprotein convertases represses the metastatic potential of human colorectal tumor cells. *J Clin Invest* **118**, 352–363.

[32] Lapierre M, Siegfried G, Scamuffa N, Bontemps Y, Calvo F, Seidah NG, and Khatib AM (2007). Opposing function of the proprotein convertases furin and PACE4 on breast cancer cells' malignant phenotypes: role of tissue inhibitors of metalloproteinase-1. *Cancer Res* **67**, 9030–9034.

[33] Basak A, Khatib AM, Mohottalage D, Basak S, Kolajova M, and Bag SS (2009). A novel enediynyl peptide inhibitor of furin that blocks processing of proPDGF-A, B and proVEGF-C. *PLoS One* **4**, e7700.

[34] Mercapide J, Lopez De Cicco R, Bassi DE, Castresana JS, Thomas G, and Klein-Szanto AJ (2002). Inhibition of furin-mediated processing results in suppression of astrocytoma cell growth and invasiveness. *Clin Cancer Res* **8**, 1740–1746.

[35] Bassi DE, Lopez De Cicco R, Cenna J, Litwin S, Cukierman E, and Klein-Szanto AJ (2005). PACE4 expression in mouse basal keratinocytes results in basement membrane disruption and acceleration of tumor progression. *Cancer Res* **65**, 7310–7319.

[36] Cheng M, Watson PH, Paterson JA, Seidah N, Chretien M, and Shiu RP (1997). Pro-protein convertase gene expression in human breast cancer. *Int J Cancer* **71**, 966–971.

[37] Ruggeri B, Caamano J, Slaga TJ, Conti CJ, Nelson WJ, and Klein-Szanto AJ (1992). Alterations in the expression of uvomorulin and Na+,K(+)-adenosine triphosphatase during mouse skin tumor progression. *Am J Pathol* **140**, 1179–1185.

[38] Lichti U, Anders J, and Yuspa SH (2008). Isolation and short-term culture of primary keratinocytes, hair follicle populations and dermal cells from newborn mice and keratinocytes from adult mice for *in vitro* analysis and for grafting to immunodeficient mice. *Nat Protoc* **3**, 799–810.

[39] Charpentier E, Lavker RM, Acquista E, and Cowin P (2000). Plakoglobin suppresses epithelial proliferation and hair growth *in vivo*. *J Cell Biol* **149**, 503–520.

[40] Fu J, Jin F, Zhang J, Fong K, Bassi DE, Lopez De Cicco R, Ramaraju D, Braunewell KH, Conti C, Benavides F, et al. (2010). VILIP-1 expression *in vivo* results in decreased mouse skin keratinocyte proliferation and tumor development. *PLoS One* **5**, e10196.

[41] Mahloogi H, Gonzalez-Guerrico AM, Lopez De Cicco R, Bassi DE, Goodrow T, Braunewell KH, and Klein-Szanto AJ (2003). Overexpression of the calcium sensor visinin-like protein-1 leads to a cAMP-mediated decrease of *in vivo* and *in vitro* growth and invasiveness of squamous cell carcinoma cells. *Cancer Res* **63**, 4997–5004.

[42] Lopez De Cicco R, Bassi DE, Page R, and Klein-Szanto AJ (2002). Furin expression in squamous cell carcinomas of the oral cavity and other sites evaluated by tissue microarray technology. *Acta Odontol Latinoam* **15**, 29–37.

[43] Page RE, Klein-Szanto AJ, Litwin S, Nicolas E, Al-Jumaily R, Alexander P, Godwin AK, Ross EA, Schilder RJ, and Bassi DE (2007). Increased expression of the pro-protein convertase furin predicts decreased survival in ovarian cancer. *Cell Oncol* **29**, 289–299.

[44] Bassi DE, Zhang J, Cenna J, Litwin S, Cukierman E, and Klein-Szanto AJ (2010). Proprotein convertase inhibition results in decreased skin cell proliferation, tumorigenesis, and metastasis. *Neoplasia* **12**, 516–526.

[45] Blanchette F, Day R, Dong W, Laprise MH, and Dubois CM (1997). TGFβ1 regulates gene expression of its own converting enzyme furin. *J Clin Invest* **99**, 1974–1983.

[46] Dubois CM, Blanchette F, Laprise MH, Leduc R, Grondin F, and Seidah NG (2001). Evidence that furin is an authentic transforming growth factor-β1–converting enzyme. *Am J Pathol* **158**, 305–316.

[47] Lopez De Cicco R, Watson JC, Bassi DE, Litwin S, and Klein-Szanto AJ (2004). Simultaneous expression of furin and vascular endothelial growth factor in human oral tongue squamous cell carcinoma progression. *Clin Cancer Res* **10**, 4480–4488.

[48] Lapouge G, Youssef KK, Vokaer B, Achouri Y, Michaux C, Sotiropoulou PA, and Blanpain C (2011). Identifying the cellular origin of squamous skin tumors. *Proc Natl Acad Sci USA* **108**, 7431–7436.

[49] Morris RJ, Tryson KA, and Wu KQ (2000). Evidence that the epidermal targets of carcinogen action are found in the interfollicular epidermis of infundibulum as well as in the hair follicles. *Cancer Res* **60**, 226–229.

[50] Hansen LA and Tennant RW (1994). Follicular origin of epidermal papillomas in v-Ha-*ras* transgenic TG.AC mouse skin. *Proc Natl Acad Sci USA* **91**, 7822–7826.

[51] Scopsi L, Gullo M, Rilke F, Martin S, and Steiner DF (1995). Proprotein convertases (PC1/PC3 and PC2) in normal and neoplastic human tissues: their use as markers of neuroendocrine differentiation. *J Clin Endocrinol Metab* **80**, 294–301.